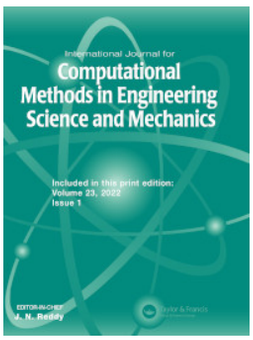

International Journal for Computational Methods in Engineering Science and Mechanics

ISSN: (Print) (Online) Journal homepage: https://www.tandfonline.com/loi/ucme20

Performance of the multigrid method with time-stepping to solve 1D and 2D wave equations

Maicon F. Malacarne, Marcio A. V. Pinto & Sebastião R. Franco

To cite this article: Maicon F. Malacarne, Marcio A. V. Pinto & Sebastião R. Franco (2022) Performance of the multigrid method with time-stepping to solve 1D and 2D wave equations, International Journal for Computational Methods in Engineering Science and Mechanics, 23:1, 45-56, DOI: 10.1080/15502287.2021.1910750

To link to this article: https://doi.org/10.1080/15502287.2021.1910750

Published online: 15 Apr 2021.

INTERNATIONAL JOURNAL FOR COMPUTATIONAL METHODS IN ENGINEERING SCIENCE AND MECHANICS
2022, VOL. 23, NO. 1, 45–56
https://doi.org/10.1080/15502287.2021.1910750

Performance of the multigrid method with time-stepping to solve 1D and 2D wave equations

Maicon F. Malacarne[a], Marcio A. V. Pinto[b], and Sebastião R. Franco[c]

[a]Graduate Program on Numerical Methods in Engineering – PPGMNE, Federal University of Parana – UFPR, Curitiba, PR, Brazil; [b]Department of Mechanical Engineering, Federal University of Parana – UFPR, Curitiba, PR, Brazil; [c]Department of Mathematics, State University of Centro-Oeste – UNICENTRO, Irati, PR, Brazil

ABSTRACT

This work aims to discuss a proposed solution for wave equations that utilize discretization by means of the finite difference method, weighted by a parameter η, with sweeping done according to the time-stepping method. The multigrid method is employed to speed up the convergence in obtaining the solution of the system of equations resulting from the discretization. To validate the proposed model, the discretization errors, effective and apparent orders, convergence factor, orders of complexity, and the computational time were assessed. A comparison between the singlegrid and multigrid methods was carried out in order to determine the most advantageous one.

KEYWORDS

Complexity order; finite difference method; speed-up; convergence; wave equation; multigrid

1. Introduction

Partial differential equations (PDEs) are used to model several engineering problems. These equations must to respect certain boundary and initial (in the transient case) conditions, in which the obtention of an analytical solution is an arduous and not always possible task. In this context, approximate methods emerge, offering the conditions of representing continuous domains as discrete domains. Led by computational advancement and the development of new technologies, the possibility of solving more realistic problems becomes more feasible.

In this work, we present a model to solve the wave equation, which is a hyperbolic PDE. This class of problem is a trendy research topic and has several applications. Some applications include structural acoustics in Avalos and Lasiecka [1], propagation of electrical charges in Metaxas and Meredith [2] and sound waves in Bailly and Juve [3], wave equation in polar coordinates in Gopal et al. [4], stationary wave equations in Brandt and Livishits [5], telegraph equation in Devi et al. [6], linear cases in Dehgham and Mohebbi [7], nonlinear cases in Rincon and Quintino [8] and Baskonus et al. [9], systems of advection equations in De Sterck et al. [10] and parallelization schemes in Gander et al. [11] and [12].

The transient wave equation is discretized by the finite difference method [13] and generates a linear system that can be solved by a solver, such as Gauss–Seidel method. One way to speed up the process of obtaining the solution of this system is to apply the multigrid method, widely recommended in the literature, as it significantly improves the convergence factor [14–16]. The anisotropy related to the physical and numerical factors of this type of problem is also evaluated. Is a challenge to solve wave equations with a high value of α, where alpha is associated with the wave propagation speed, see Umenati et al. [17].

When solving physical problems modeled by PDEs that are dependent on time, the time-stepping technique can be used, in which, at each new time step, the solution of the previous time step is utilized as an initial estimate, thus solving a transient problem with a system of stationary wave equations [18–21]. Time-stepping is usually proposed to solve elliptical and parabolic problems [22], but it can also be employed in the wave equation [7]. To calculate the approximate solution at the current time step in the wave equation, we use the solutions of the two previous time steps.

This work is organized as follows. In Section 2, we present the mathematical models adopted for the wave equation and discretization for the 1D and 2D

CONTACT Maicon F. Malacarne maicon.unicentro@hotmail.com Graduate Program on Numerical Methods in Engineering – PPGMNE, Federal University of Parana – UFPR, Cel. Francisco H. dos Santos Ave, 100 – Jardim das Américas, 81530-000 Curitiba, PR, Brazil.

cases. In Section 3, we show details of the implementation of the multigrid method in the wave equation. In Section 4, we expose the code verification methods and the results of the simulations. Finally, in Section 5, we present the conclusions.

2. Mathematical and numerical models

2.1. One-dimensional wave equation

The 1D wave equation can be utilized to model, for instance, the problem of a vibrating string fixed at both ends, in which the goal is to find the displacement $u(x, t)$ with the independent variables x and t, which represent, respectively, the position and time. Let α_1 be a scalar which is a positive real number defined as $\alpha_1^2 = \frac{1}{V_1^2}$, where V_1 is related to the linear density and the tension of the string (wave propagation speed). Let us consider the one-dimensional wave equation [23] as

$$\frac{\partial^2 u}{\partial t^2} = \alpha_1^2 \frac{\partial^2 u}{\partial x^2}, \tag{1}$$

$$u(x,0) = f_1(x), \quad 0 \le x \le l, \tag{2}$$

$$u_t(x,0) = g_1(x), \quad 0 \le x \le l, \tag{3}$$

$$u(0,t) = u(l,t) = 0, \quad t > 0, \tag{4}$$

where $f_1(x)$ represents the initial setup, $g_1(x)$ is the initial speed, and $u(0, t)$ and $u(l, t)$ are the boundary conditions. The general solution is built with the fundamental vibrational frequencies given by varying $n = 1, 2, 3, \ldots$, such as

$$u(x,t) = \sum_{n=1}^{\infty} (c_n w_n^0(x,t) + d_n z_n^0(x,t)) \tag{5}$$

where

$$w_n^0(x,t) = \cos\left(\frac{n\pi\alpha_1 t}{l}\right) \sin\left(\frac{n\pi x}{l}\right), \tag{6}$$

$$z_n^0(x,t) = \sin\left(\frac{n\pi\alpha_1 t}{l}\right) \sin\left(\frac{n\pi x}{l}\right), \tag{7}$$

$$c_n = \frac{2}{l}\int_0^l f_1(x) \sin\left(\frac{n\pi x}{l}\right) dx, \tag{8}$$

$$d_n = \frac{2}{n\pi\alpha_1}\int_0^l g_1(x) \sin\left(\frac{n\pi x}{l}\right) dx, \tag{9}$$

2.2. Discretization wave 1D

Considering the problem defined in Eqs. (1)–(4), we define the size of each spatial element $h_1 = \frac{l}{N_x}$, and a time increment $\tau_1 = \frac{t_f}{N_t}$, where $N_x > 0$ and $N_t > 0$ are the numbers of spatial and temporal intervals, respectively, with time $t_f > 0$ and string length l. By admitting an approximation v_i^k for the solution u, at a point of coordinate x_i, with time k, and using central difference, the discretized problem is given by

$$\begin{aligned}
&\frac{v_i^{k-1} - 2v_i^k + v_i^{k+1}}{\tau_1^2} - \frac{\tau_1^2}{12}\frac{\partial^4 v_i}{\partial t^4} - \frac{\tau_1^4}{360}\frac{\partial^6 v_i}{\partial t^6} - \frac{\tau_1^6}{20160}\frac{\partial^8 v_i}{\partial t^8} - \cdots = \\
&\alpha_1^2\eta_1\left(\frac{v_{i-1}^{k+1} - 2v_i^{k+1} + v_{i+1}^{k+1}}{h_1^2} - \frac{h_1^2}{12}\frac{\partial^4 v_i^{k+1}}{\partial x^4} - \frac{h_1^4}{360}\frac{\partial^6 v_i^{k+1}}{\partial x^6} - \frac{h_1^6}{20160}\frac{\partial^8 v_i^{k+1}}{\partial x^8} - \cdots\right) \\
&+\alpha_1^2(1-2\eta_1)\left(\frac{v_{i-1}^{k} - 2v_i^{k} + v_{i+1}^{k}}{h_1^2} - \frac{h_1^2}{12}\frac{\partial^4 v_i^{k}}{\partial x^4} - \frac{h_1^4}{360}\frac{\partial^6 v_i^{k}}{\partial x^6} - \frac{h_1^6}{20160}\frac{\partial^8 v_i^{k}}{\partial x^8} - \cdots\right) \\
&+\alpha_1^2\eta_1\left(\frac{v_{i-1}^{k-1} - 2v_i^{k-1} + v_{i+1}^{k-1}}{h_1^2} - \frac{h_1^2}{12}\frac{\partial^4 v_i^{k-1}}{\partial x^4} - \frac{h_1^4}{360}\frac{\partial^6 v_i^{k-1}}{\partial x^6} - \frac{h_1^6}{20160}\frac{\partial^8 v_i^{k-1}}{\partial x^8} - \cdots\right),
\end{aligned} \tag{10}$$

where η_1 is the weighting parameter. By adopting $\eta_1 > 0.25$, we have an unconditionally stable approach [13]. By rearranging the terms of Eq. (10), we have

$$\begin{aligned}
v_i^{k-1} - 2v_i^k + v_i^{k+1} = \frac{\alpha_1^2\tau_1^2}{h_1^2}[&\eta_1(v_{i-1}^{k+1} - 2v_i^{k+1} + v_{i+1}^{k+1}) \\
&+ (1-2\eta_1)(v_{i-1}^{k} - 2v_i^{k} + v_{i+1}^{k}) \\
&+ \eta_1(v_{i-1}^{k-1} - 2v_i^{k-1} + v_{i+1}^{k-1})]
\end{aligned} \tag{11}$$

with truncation error order $O(h_1^2\tau_1^2, \tau_1^4)$, given by

$$\begin{aligned}
\varepsilon_{1D} = &+\frac{\tau_1^4}{12}\frac{\partial^4 v_i}{\partial t^4} + \cdots - \frac{\alpha_1^2\tau_1^2 h_1^2\eta_1}{12}\frac{\partial^4 v_i^{k+1}}{\partial x^4} - \cdots \\
&- \frac{\alpha_1^2\tau_1^2 h_1^2}{12}(1-2\eta_1)\frac{\partial^4 v_i^k}{\partial x^4} - \\
&\cdots - \frac{\alpha_1^2\tau_1^2 h_1^2\eta_1}{12}\frac{\partial^4 v_i^{k-1}}{\partial x^4} - \cdots
\end{aligned} \tag{12}$$

Assuming that,

$$\lambda_1 = \frac{\alpha_1^2\tau_1^2}{h_1^2}, \tag{13}$$

we have

$$\begin{aligned}
(1+2\eta_1\lambda_1)v_i^{k+1} = &\eta_1\lambda_1(v_{i-1}^{k+1} + v_{i+1}^{k+1}) + (-1-2\eta_1\lambda_1)v_i^{k-1} \\
&+ (2 + (-2+4\eta_1)\lambda_1)v_i^k \\
&+ (1-2\eta_1)\lambda_1(v_{i-1}^k + v_{i+1}^k) \\
&+ \eta_1\lambda_1(v_{i-1}^{k-1} + v_{i+1}^{k-1}).
\end{aligned} \tag{14}$$

Therefore, we have the coefficients and source term given by

$$a_{p1} = 1 + 2\eta_1\lambda_1, \tag{15}$$

$$a_{w1} = a_{e1} = \eta_1\lambda_1, \tag{16}$$

$$\begin{aligned}
b_{p1} = &(-1-2\eta_1\lambda_1)v_i^{k-1} + (2 + (-2+4\eta_1)\lambda_1)v_i^k \\
&+ (1-2\eta_1)\lambda_1(v_{i-1}^k + v_{i+1}^k) + \eta_1\lambda_1(v_{i-1}^{k-1} + v_{i+1}^{k-1}).
\end{aligned} \tag{17}$$

In order to perform the iteration is necessary to know the solution at two time-steps before, v_i^k and v_i^{k-1}. To start the process, v_i^{k-1} is given by the initial setup and v_i^k is given, as in Burden and Faires [24], by

$$v_i^k = (1-\lambda_1)f_1(x_i) + \frac{\lambda_1}{2}f_1(x_{i+1}) + \frac{\lambda_1}{2}f_1(x_{i-1}) + \tau_1 g_1(x_i) + O(h_1^2\tau_1^2). \tag{18}$$

2.3. Two-dimensional wave equation

The two-dimensional wave equation can be utilized to model, for example, the problem of a vibrating rectangular membrane with fixed edges, in which the intention is to find the displacement $u(x,y,t)$, with independent variables $0<x<l_x$ and $0<y<l_y$, which represent the plane's spatial coordinates, for the time $t>0$. Assume that α_2^2 is a positive real number $\alpha_2^2 = \frac{1}{V_2^2}$, where V_2 is related to the superficial density and local tension, we define the two-dimensional wave equation [23] as

$$\frac{\partial^2 u}{\partial t^2} = \alpha_2^2\left(\frac{\partial^2 u}{\partial x^2} + \frac{\partial^2 u}{\partial y^2}\right), \tag{19}$$

$$u(x,y,0) = f_2(x,y), \tag{20}$$

$$u_t(x,y,0) = g_2(x,y), \tag{21}$$

$$u(x,0,t) = u(x,l_y,t) = u(0,y,t) = u(l_x,y,t) = 0, \quad t>0 \tag{22}$$

where $f_2(x,y)$ is the initial setup, $g_2(x,y)$ is the initial speed, $u(x,0,t), u(x,l_y,t), u(0,y,t)$, and $u(l_x,y,t)$ represent the boundary conditions. In this case, the general solution is built with the fundamental vibrational frequencies that are given by varying $m = 1,2,3,\ldots, n = 1,2,3,\ldots$, and it is given by

$$u(x,y,t) = \sum_{m=1}^{\infty}\sum_{n=1}^{\infty}(a_{m,n}w^1_{m,n}(x,y,t) + b_{m,n}z^1_{m,n}(x,y,t)), \tag{23}$$

where

$$w^1_{m,n}(x,y,t) = \cos\left(\pi\alpha_2\sqrt{\frac{m^2}{l_x^2}+\frac{n^2}{l_y^2}}t\right)\sin\left(\frac{m\pi x}{l_x}\right)\sin\left(\frac{n\pi y}{l_y}\right), \tag{24}$$

$$z^1_{m,n}(x,y,t) = \sin\left(\pi\alpha_2\sqrt{\frac{m^2}{l_x^2}+\frac{n^2}{l_y^2}}t\right)\sin\left(\frac{m\pi x}{l_x}\right)\sin\left(\frac{n\pi y}{l_y}\right), \tag{25}$$

$$a_{m,n} = \frac{4}{l_x l_y}\int_0^{l_y}\int_0^{l_x} f_2(x,y)\sin\left(\frac{m\pi x}{l_x}\right)\sin\left(\frac{n\pi y}{l_y}\right)dxdy, \tag{26}$$

$$b_{m,n} = \frac{4}{\pi\alpha_2\sqrt{m^2l_y^2+n^2l_x^2}}\int_0^{l_y}\int_0^{l_x} g_2(x,y)\sin\left(\frac{m\pi x}{l_x}\right)\sin\left(\frac{n\pi y}{l_y}\right)dxdy. \tag{27}$$

2.4. Discretization wave 2D

Considering the problem defined in Eqs. (19)–(22), and a rectangular membrane of side L, that is, $l_x = l_y = L$, we define the size of each spatial element by $h_x = \frac{L}{N_x}$ and $h_y = \frac{L}{N_y}$, and a time increment by $\tau_2 = \frac{t_f}{N_t}$, where N_x, N_y, and N_t are the numbers of the spatial and temporal intervals, respectively, with a time $t_f > 0$. By admitting an approximation $v_{i,j}^k$ for the solution u, at a point of coordinates (x_i, y_j), with time k, and utilizing central difference scheme, the two-dimensional problem can be discretized with finite difference methods, expanding the methodology employed for the one-dimensional case. Thus, we have

$$\begin{aligned}
&\frac{v_{i,j}^{k-1}-2v_{i,j}^k+v_{i,j}^{k+1}}{\tau_2^2} - \frac{\tau_2^2}{12}\frac{\partial^4 v_{i,j}}{\partial t^4} - \frac{\tau_2^4}{360}\frac{\partial^6 v_{i,j}}{\partial t^6} - \frac{\tau_2^6}{20160}\frac{\partial^8 v_{i,j}}{\partial t^8} - \cdots = \\
&\alpha_2^2\eta_2\left(\frac{(v_{i-1,j}^{k+1}-2v_{i,j}^{k+1}+v_{i+1,j}^{k+1})}{h_x^2} - \frac{h_x^2}{12}\frac{\partial^4 v_{i,j}^{k+1}}{\partial x^4} - \frac{h_x^4}{360}\frac{\partial^6 v_{i,j}^{k+1}}{\partial x^6} - \frac{h_x^6}{20160}\frac{\partial^8 v_{i,j}^{k+1}}{\partial x^8} - \cdots\right) \\
&+\alpha_2^2(1-2\eta_2)\left(\frac{(v_{i-1,j}^{k}-2v_{i,j}^{k}+v_{i+1,j}^{k})}{h_x^2} - \frac{h_x^2}{12}\frac{\partial^4 v_{i,j}^{k}}{\partial x^4} - \frac{h_x^4}{360}\frac{\partial^6 v_{i,j}^{k}}{\partial x^6} - \frac{h_x^6}{20160}\frac{\partial^8 v_{i,j}^{k}}{\partial x^8} - \cdots\right) \\
&+\alpha_2^2\eta_2\left(\frac{(v_{i-1,j}^{k-1}-2v_{i,j}^{k-1}+v_{i+1,j}^{k-1})}{h_x^2} - \frac{h_x^2}{12}\frac{\partial^4 v_{i,j}^{k-1}}{\partial x^4} - \frac{h_x^4}{360}\frac{\partial^6 v_{i,j}^{k-1}}{\partial x^6} - \frac{h_x^6}{20160}\frac{\partial^8 v_{i,j}^{k-1}}{\partial x^8} - \cdots\right) \\
&+\alpha_2^2\eta_2\left(\frac{(v_{i,j-1}^{k+1}-2v_{i,j}^{k+1}+v_{i,j+1}^{k+1})}{h_y^2} - \frac{h_y^2}{12}\frac{\partial^4 v_{i,j}^{k+1}}{\partial y^4} - \frac{h_y^4}{360}\frac{\partial^6 v_{i,j}^{k+1}}{\partial y^6} - \frac{h_y^6}{20160}\frac{\partial^8 v_{i,j}^{k+1}}{\partial y^8} - \cdots\right) \\
&+\alpha_2^2(1-2\eta_2)\left(\frac{(v_{i,j-1}^{k}-2v_{i,j}^{k}+v_{i,j+1}^{k})}{h_y^2} - \frac{h_y^2}{12}\frac{\partial^4 v_{i,j}^{k}}{\partial y^4} - \frac{h_y^4}{360}\frac{\partial^6 v_{i,j}^{k}}{\partial y^6} - \frac{h_y^6}{20160}\frac{\partial^8 v_{i,j}^{k}}{\partial y^8} - \cdots\right) \\
&+\alpha_2^2\eta_2\left(\frac{(v_{i,j-1}^{k-1}-2v_{i,j}^{k-1}+v_{i,j+1}^{k-1})}{h_y^2} - \frac{h_y^2}{12}\frac{\partial^4 v_{i,j}^{k-1}}{\partial y^4} - \frac{h_y^4}{360}\frac{\partial^6 v_{i,j}^{k-1}}{\partial y^6} - \frac{h_y^6}{20160}\frac{\partial^8 v_{i,j}^{k-1}}{\partial y^8} - \cdots\right)
\end{aligned} \tag{28}$$

Assuming $h_2 = h_x = h_y$ and rearranging the terms of the previous equation, we obtain

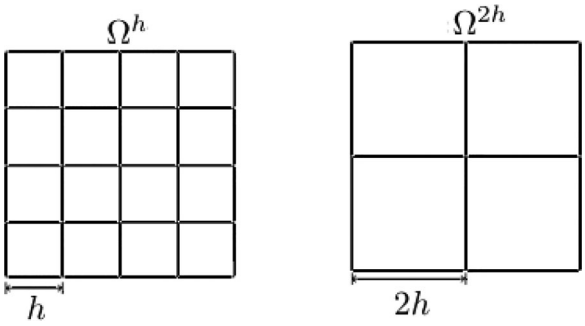

Figure 1. Coarsening ratio.

$$\begin{aligned} v_{i,j}^{k-1} - 2v_{i,j}^{k} + v_{i,j}^{k+1} = \frac{\alpha_2^2\tau_2^2}{h_2^2}\Big[&(v_{i-1,j}^{k+1} + v_{i,j-1}^{k+1} \\ &- 4v_{i,j}^{k+1} + v_{i+1,j}^{k+1} + v_{i,j+1}^{k+1}) \\ &+ (1-2\eta_2)(v_{i-1,j}^{k} + v_{i,j-1}^{k} - 4v_{i,j}^{k} + v_{i+1,j}^{k} + v_{i,j+1}^{k}) \\ &+ \eta_2(v_{i-1,j}^{k-1} + v_{i,j-1}^{k-1} - 4v_{i,j}^{k-1} + v_{i+1,j}^{k-1} + v_{i,j+1}^{k-1})\Big]. \end{aligned} \tag{29}$$

with truncation error order $O(h_x^2\tau_2^2, h_y^2\tau_2^2, \tau_2^4)$, given by

$$\begin{aligned} \varepsilon_{2D} = &+\frac{\tau_2^4}{12}\frac{\partial^4 v_{i,j}}{\partial t^4} + \cdots - \frac{\alpha_2^2\tau_2^2h_x^2\eta_2}{12}\frac{\partial^4 v_{i,j}^{k+1}}{\partial x^4} - \cdots \\ &- \frac{\alpha_2^2\tau_2^2h_x^2}{12}(1-2\eta_2)\frac{\partial^4 v_{i,j}^{k}}{\partial x^4} - \cdots \\ &- \frac{\alpha_2^2\tau_2^2h_x^2\eta_2}{12}\frac{\partial^4 v_{i,j}^{k-1}}{\partial x^4} - \cdots - \frac{\alpha_2^2\tau_2^2h_y^2\eta_2}{12}\frac{\partial^4 v_{i,j}^{k+1}}{\partial y^4} \\ &- \cdots - \frac{\alpha_2^2\tau_2^2h_y^2}{12}(1-2\eta_2)\frac{\partial^4 v_{i,j}^{k}}{\partial y^4} - \cdots \\ &- \frac{\alpha_2^2\tau_2^2h_y^2\eta_2}{12}\frac{\partial^4 v_{i,j}^{k-1}}{\partial y^4} - \cdots \end{aligned} \tag{30}$$

Assuming that,

$$\lambda_2 = \frac{\alpha_2^2\tau_2^2}{h_2^2}, \tag{31}$$

we have

$$\begin{aligned} (1+4\eta_2\lambda_2)v_{i,j}^{k+1} = &\ \eta_2\lambda_2(v_{i-1,j}^{k+1} + v_{i+1,j}^{k+1} + v_{i,j-1}^{k+1} + v_{i,j+1}^{k+1}) \\ &+ \lambda_2\Big[(1-2\eta_2)(v_{i-1,j}^{k} + v_{i+1,j}^{k} + v_{i,j-1}^{k} \\ &+ v_{i,j+1}^{k}) + \eta_2(v_{i-1,j}^{k-1} + v_{i+1,j}^{k-1} + v_{i,j-1}^{k-1} + v_{i,j+1}^{k-1})\Big] \\ &+ [2 - 4\lambda_2 + 8\eta_2\lambda_2]v_{i,j}^{k} + [-1 - 4\eta_2\lambda_2]v_{i,j}^{k-1}, \end{aligned} \tag{32}$$

Therefore, we obtain the coefficients and the source term given by

$$a_{p2} = 1 + 4\eta_2\lambda_2, \tag{33}$$

$$a_{w2} = a_{e2} = a_{s2} = a_{n2} = \eta_2\lambda_2, \tag{34}$$

$$\begin{aligned} b_{p2} = \lambda_2\Big[&(1-2\eta_2)(v_{i-1,j}^{k} + v_{i+1,j}^{k} + v_{i,j-1}^{k} + v_{i,j+1}^{k}) \\ &+ \eta_2(v_{i-1,j}^{k-1} + v_{i+1,j}^{k-1} + v_{i,j-1}^{k-1} + v_{i,j+1}^{k-1})] + \\ &(2 - 4\lambda_2 + 8\eta_2\lambda_2)v_{i,j}^{k} + (-1 - 4\eta_2\lambda_2)v_{i,j}^{k-1}. \end{aligned} \tag{35}$$

In order to compute $v_{i,j}^{k+1}$, it is necessary to know the solutions of the two previous time steps, $v_{i,j}^{k}$ and $v_{i,j}^{k-1}$. To initiate the process, $v_{i,j}^{k-1}$ is given by the initial setup and $v_{i,j}^{k}$ is calculated with central differencing scheme by Eq. (36)

$$\begin{aligned} v_{i,j}^{k} = &(1-\lambda_2)f_2(x_i, y_j) \\ &+ \frac{\lambda_2}{2}[f_2(x_i, y_{j+1}) + f_2(x_i, y_{j-1}) + f_2(x_{i-1}, y_j) \\ &+ f_2(x_{i+1}, y_j)] + \tau_2 g_2(x_i, y_j) + O(h_2^2). \end{aligned} \tag{36}$$

3. Multigrid method

The multigrid method is employed to accelerate the convergence when obtaining the solution of the resulting system of equations since it is possible to smooth oscillatory components at each grid when using a set of grids [14] and [25]. This technique is commonly used by researchers when solving a system of equations of the type $Au = f$, which usually demands a high computational cost [26–29]. In this case, we define $r^{it} = f - Av^{it}$, as being the residual generated by v in the iteration it, where v is an approximation.

The multigrid deals with a basic iterative method, called smoother, to smooth high and low-frequency errors. This is possible due to the use of several grids, since components that are smooth at finer grids become more oscillatory at coarser grids [14] and [30].

The order in which the different grids are visited is called the multigrid cycle. In this work, we use the V-cycle, shown in more detail in the sequence, and proposed in the works of Briggs et al. [16] and Trottenberg et al. [14]. In the V-cycle, the equation is smoothed ν_1 times (pre-smoothing) at the finer grid; hence, the residual is transferred to the very next coarser grid by means of restriction operators I_h^{2h}, with full-weighting for the 1D problem and half-weighting for the 2D problem, represented respectively in Eqs. (37) and (38):

$$r_{2h}(x_i) = I_h^{2h}r_h(x_i) = \frac{1}{4}[2r_h(x_i) + r_h(x_{i+1}) + r_h(x_{i-1})], \tag{37}$$

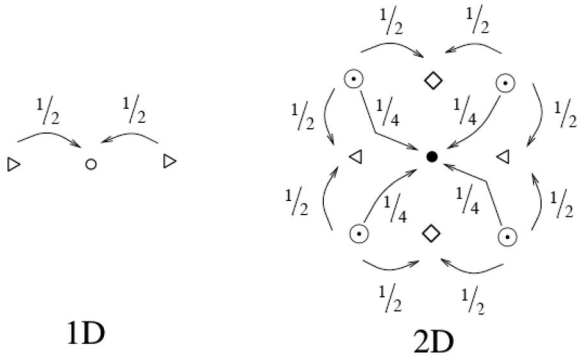

Figure 2. Linear and bilinear interpolation.

$$r_{2h}(x_i,y_j) = I_h^{2h} r_h(x_i,y_j) = \frac{1}{8}[4r_h(x_i,y_j) + r_h(x_{i+1},y_j) + r_h(x_{i-1},y_j) + r_h(x_i,y_{j+1}) + r_h(x_i,y_{j-1})], \tag{38}$$

where r_h and r_{2h} are, respectively, the residuals of the fine and coarse grids. In this work, we use the standard coarsening ratio, $q = 2$ [14], given by $q = H/h$, where h and H represent the size of the fine grid and its immediately coarser grid, respectively. This type of coarsening is depicted in Figure 1, for the two-dimensional problem. This process is repeated until the coarsest grid is reached, and thus the problem is solved.

Then, the prolongation of the corrections is performed, using linear interpolation operators I_{2h}^h in the 1D problem and bilinear interpolation operations in the 2D problem, given respectively by Eqs. (39) and (40):

$$v_h(x_i) = I_{2h}^h v_h(x_i) = \begin{cases} \frac{1}{2}[v_{2h}(x_{i-1}) + v_{2h}(x_{i+1})], & \text{for } \circ, \\ v_{2h}(x_i), & \text{for } \triangleright, \end{cases} \tag{39}$$

$$v_h(x_i,y_j) = I_{2h}^h v_h(x_i,y_j) = \begin{cases} \frac{1}{2}\left[v_{2h}(x_{i-1},y_j) + v_{2h}(x_{i+1},y_j)\right], & \text{for } \diamond, \\ \frac{1}{2}\left[v_{2h}(x_i,y_{j-1}) + v_{2h}(x_i,y_{j+1})\right], & \text{for } \triangleleft, \\ \frac{1}{4}[v_{2h}(x_{i-1},y_j) + v_{2h}(x_{i+1},y_j) + v_{2h}(x_i,y_{j-1}) + v_{2h}(x_i,y_{j+1})], & \text{for } \bullet, \\ v_{2h}(x_i,y_j), & \text{for } \odot, \end{cases} \tag{40}$$

Figure 2 shows images of the interpolators of Eqs. (39) and (40) [14], where the points $\triangleright$ and $\odot$ are seen on fine Ω^h and coarse Ω^{2h} grids, whereas the points $\circ$, $\diamond$, $\triangleleft$, and $\bullet$ are seen only on the fine grid Ω^h.

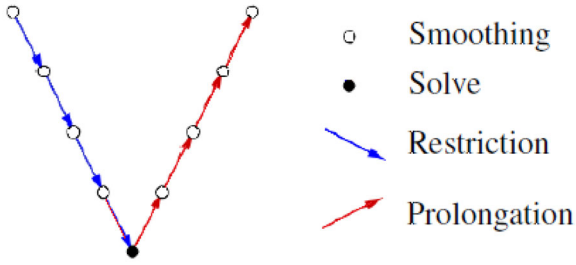

Figure 3. Multigrid V-cycle.

The solution is then corrected and smoothed ν_2 times (post-smoothing), and the process is repeated until the finest grid Ω^h is reached, where the solution is smoothed one more time [16] and [31]. This process is depicted in Figure 3.

The V-cycle is repeated until the stop criterion is met. This approach allows the iterative process of the multigrid method to always smooth oscillatory components [32]. We adopt $\nu_1 = \nu_2 = 2$ in this work, as according to Dehgan and Mohebbi [7], this choice yields positive results for the wave equation.

4. Results

In this section, we discuss the code verification techniques based on the numerical simulations and also on *a posteriori* analysis of the results found with the multigrid and singlegrid formulations, using Gauss–Seidel as smoother and lexicographical order [33]. Tests were performed in an Intel Core i3 1.5 GHz computer, 4 GB Ram, 64-bits, Windows 10 operating system, and double precision.

The 1D problem, modeled by Eqs. (1)–(4), is solved by admitting $\alpha_1 = 2$, initial setup $f_1(x) = \sin(\pi x)$ and initial speed $g_1(x) = 0$. We adopt the same number of points in both spatial and temporal discretization $N_x = N_t$, with $\tau_1 = h_1$, parameter $\eta = 0.5$, and final time of $t_f = 1.0$s. The one-dimensional problem of a vibrating string with fixed ends is depicted in Figure 4 for a few values of t.

The 2D problem, modeled by Eqs. (19)–(22), is solved by admitting $\alpha_2 = 2$, initial setup $f_2(x,y) = \sin(\pi x)\sin(\pi y)$ and initial speed $g_2(x,y) = 0$. We adopt the same number of points in both spatial and temporal discretization $N_x = N_y = N_t$, with $\tau_2 = h_x = h_y$, parameter $\eta = 0.5$, and final time $t_f = 1.0$s. The behavior of a rectangular membrane with fixed edges is depicted in Figure 5 for a few values of t.

4.1. Discretization error

The discretization error is associated with the size of the components from the grid which is utilized. For

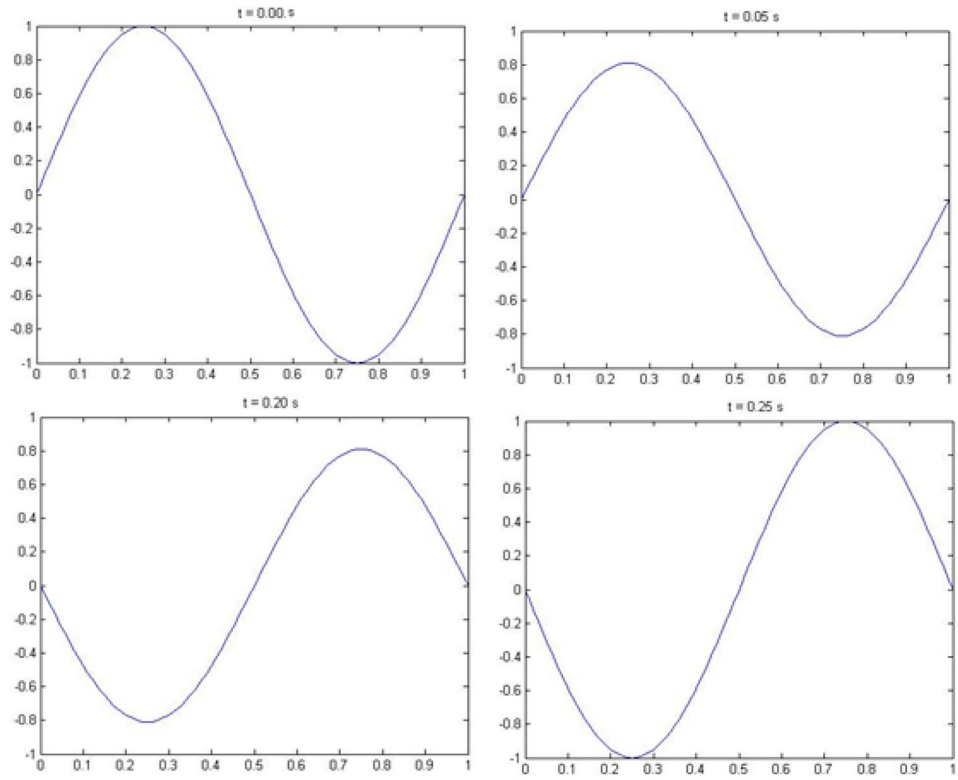

Figure 4. Vibrating string with fixed ends.

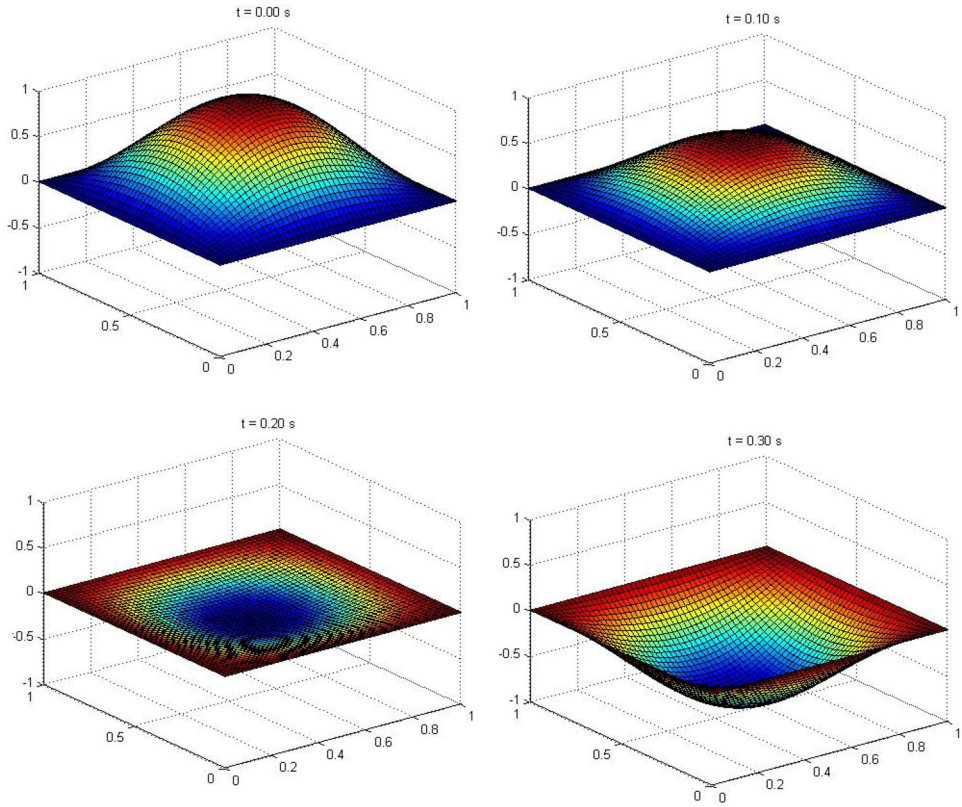

Figure 5. Behavior of a membrane with fixed edges *versus* time.

Table 1. Discretization error for different grids.

N	$\|\|E_{SG-1D}\|\|_\infty$	$\|\|E_{MG-1D}\|\|_\infty$	$\|\|E_{SG-2D}\|\|_\infty$	$\|\|E_{MG-2D}\|\|_\infty$
2^3+1	2.2247690E+00	2.2247690E+00	1.23215155E+00	1.23215155E+00
2^4+1	7.3045048E−01	7.3045048E−01	3.42788395E−01	3.42788395E−01
2^5+1	7.4352845E−02	7.4352845E−02	7.83783302E−02	7.83783302E−02
2^6+1	5.2713778E−03	5.2713778E−03	1.88555766E−02	1.88555766E−02
2^7+1	3.4245672E−04	3.4245672E−04	4.67832780E−03	4.67832780E−03
2^8+1	2.1705113E−05	2.1705113E−05	1.16979496E−03	1.16979494E−03
2^9+1	1.3643499E−06	1.3643496E−06	2.92791365E−04	2.92791376E−04

the purpose of verifying the behavior of this type of error, truncation, iterative, and roundoff errors are considered inherent. Table 1 presents the infinity norm of the numerical errors. From now on, the notation used will be: N is the number of points on the directions x, y, and t; E is the truncation error; SG and MG represent the singlegrid and multigrid methods, respectively; and 1D and 2D are the dimensions of the problem. In the first column, the number of spatial points for the 1D problem is N, and for the 2D case is N^2.

We verified a desired characteristic in both 1D and 2D approximations, the discretization error decreases as the grid is refined. Taking into account that by adopting a certain value of N, regardless of the method used, singlegrid or multigrid, the discretization error is virtually the same, given that the problem was solved up to the rounding error.

4.2. Effective and apparent orders

The order of approximation can be verified by utilizing the effective order P_E and apparent order P_U [7] and [34]. We apply the Richardson estimator based on the apparent order of the numerical error, given by

$$P_U = \frac{\log\left(\frac{\phi_2-\phi_3}{\phi_1-\phi_2}\right)}{\log(q)}, \tag{41}$$

in which ϕ_1, ϕ_2, and ϕ_3 indicate, respectively, solutions on the fine, coarse, and super coarse grids. Once the analytical solution is found, the P_E is computed by

$$P_E = \frac{\log\left(\frac{E(\phi_2)}{E(\phi_1)}\right)}{\log(q)}, \tag{42}$$

in which $E(\phi_2)$ and $E(\phi_1)$ represent the errors on the coarse and fine grids, respectively. Figure 6 shows the values of the apparent and effective orders for different grids for the 1D and 2D wave equations, with $\tau_1 = h_1$ and $\tau_2 = h_x = h_y$.

Figure 6 shows that P_U and P_E tend to 4.0, such as presented in Cuminato and Meneguette [13]. Thus, the model presented in Eqs. (10) and (18), both

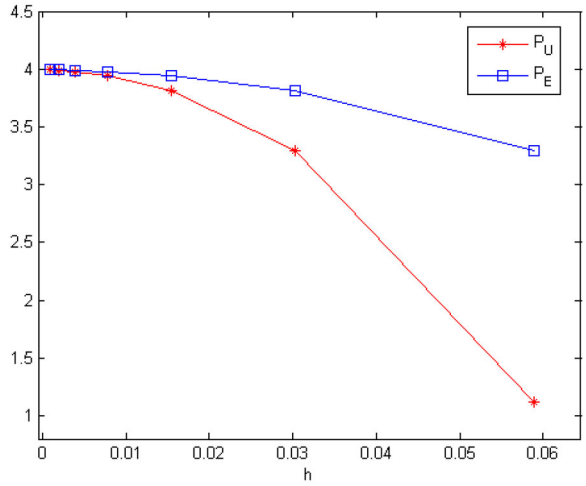

Figure 6. Apparent and effective orders for the 1D problem.

fourth-order, produce a fourth-order method for the 1D case, a desired characteristic in approximation methods. For the 2D case, in Figure 7, P_U and P_E tend to 2.0, in other words, although Eq. (28) has fourth order, Eq. (28) has second order. This combination produces a second-order method. These results are corroborated with data from Table 1.

For example, in case 1D, for $N = 2^7 + 1$ points, the error is $3.4245672E-04$ and by decreasing the size of h_1 in a half, that is, $N = 2^8 + 1$ points, the new error is $2.1705113E-05$, reducing about 16 times. But for 2D cases, by decreasing the elements size in a half, the new error reducing about 4 times.

4.3. Orders of complexity

According to Burden and Faires [24], and with the results of the computational time t_{cpu}, we can make a geometrical (or nonlinear) fit in order to assess the complexity of the algorithm utilized, where

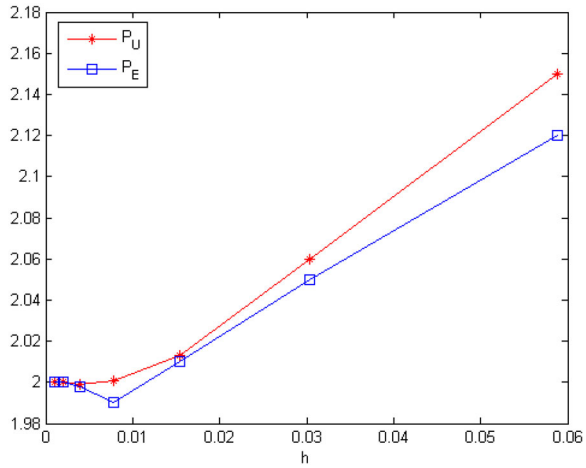

Figure 7. Apparent and effective orders for the 2D problem.

Table 2. Parameters of the geometrical fit for the 1D wave equation.

λ	c_{MG}	p_{MG}	c_{SG}	p_{SG}
10^0	1.00E − 05	0.8941	1.00E − 05	0.9723
10^1	7.00E − 06	0.9559	2.00E − 05	1.0364
10^2	2.00E − 05	0.9249	4.00E − 05	1.1175
10^3	3.00E − 05	0.9161	5.00E − 05	1.2558
10^4	4.00E − 05	0.9012	7.00E − 06	1.5312
10^5	5.00E − 05	0.9421	3.00E − 06	1.7894

Table 3. Parameters of the geometrical fit for the 2D wave equation.

λ	c_{MG}	p_{MG}	c_{SG}	p_{SG}
10^0	7.00E − 06	0.9518	1.00E − 05	0.9615
10^1	1.00E − 05	0.9438	5.00E − 05	0.9922
10^2	2.00E − 05	0.9221	1.00E − 05	1.2251
10^3	2.00E − 05	0.9341	7.00E − 07	1.5693
10^4	2.00E − 05	0.9478	2.00E − 06	1.6028
10^5	2.00E − 05	1.0071	4.00E − 07	1.7752

$$t_{cpu} = c.M^p, \tag{43}$$

in which c is the coefficient of the method, p is the order of complexity of the solver related to the inclination of the correction curve and M is the number of variables of the problem. Theoretically, Trottenberg et al. [14], p must be close to 1 for the multigrid case, showing its linear behavior. In Tables 2 and 3, we present the results of these parameters for the multigrid and singlegrid methods, for different values of λ, given by Eqs. (13) and (31), which contain information on physical aspects as α, and on numerical aspects as h and τ. From here on we will use $||r^{it}||_\infty / ||r^0||_\infty \leq 10^{-9}$ as a stopping criterion, where r^0 is residual in initial estimate.

We found a similarity between the orders of complexity of the 1D and 2D cases, as in both cases, as λ increases, p_{MG} shows values close to 1, and p_{SG} increases and tends to 2, which proves that the complexity of the multigrid method presented is linear.

4.4. Convergence factor

In order to define which interval and variable values to use in the computations, we considered the parameter λ and the convergence factor ρ, where $\rho = ||r^{it}||_\infty / ||r^{it-1}||_\infty$. According to Horton and Vandewalle [35] and Thole and Trottenberg [36], λ can be considered as a measure of the anisotropy degree at the discretized operator in a given grid, and such anisotropy can affect the performance of the solver. Since λ depends on the increase in time and space adopted in the discretization, and also on the wave propagation speed, we have a measure of physical and numerical anisotropy for the wave equation. This approach can also be used to find intervals of λ, for which multigrid and singlegrid are more efficient. This indicator is calculated for different grids, for the 1D and 2D problems, and it is shown in Figures 8 and 9, respectively.

In both cases, 1D and 2D, and for both methods, SG and MG, for values of $\log(\lambda) < 0$, we have $\rho \approx 0$, which implies a high efficiency of both methods. As $\log(\lambda)$ increases, the SG shows values of $\rho \approx 1$ for both the 1D and 2D cases, that is, SG is inefficient at this interval [32]. At this same interval, that is, $\log(\lambda) > 0$, the convergence factor of the MG method for the 1D problem shows a value of $\rho \approx 0.45$. For the 2D problem, the convergence factor of the MG method remains small, $\rho \approx 0.1$. Therefore, the multigrid method proposed for the wave equation is much

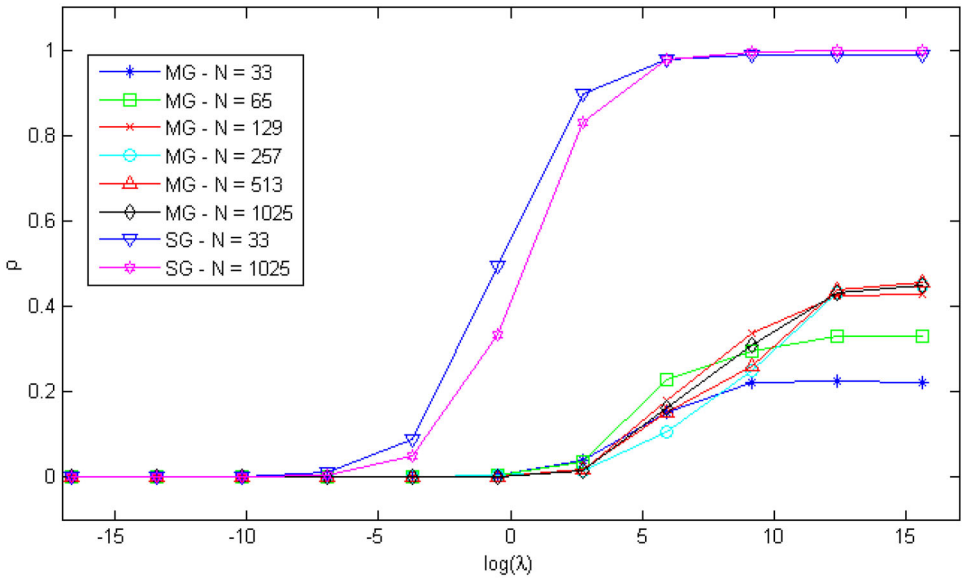

Figure 8. Convergence factor for different grids and values of λ for 1D problem.

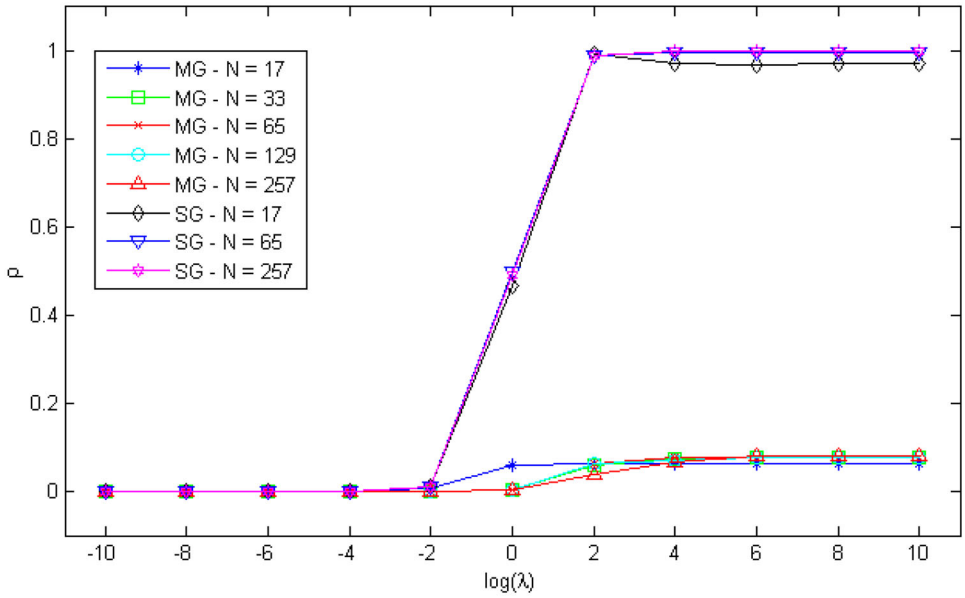

Figure 9. Convergence factor for different grids and values of λ for 2D problem.

more efficient for such values of λ. Furthermore, the values of ρ not depend on the value of λ in finer grids, showing the robustness of the method.

4.5. Speed-up

In this subsection, we found the relationship between the computational time of the singlegrid (t_{cpuSG}) and multigrid (t_{cpuMG}) and the increase in the number of points, where the speed-up $= t_{cpuSG}/t_{cpuMG}$. See Figures 10 and 11, for the 1D and 2D problems, respectively, for different values of λ.

We noticed that for both cases, 1D and 2D, the speed-up increases for higher values of N, which is desirable, and significantly increases for higher values of λ. In the 2D case, for example, for $\lambda = 10^3$ with $N = 129$, that is, with 2,048,383 unknowns, the MG method has a $t_{cpuMG} = 16.4$s and SG $t_{cpuMG} = 5291.8$s. The multigrid method solves the problem approximately 322 times faster.

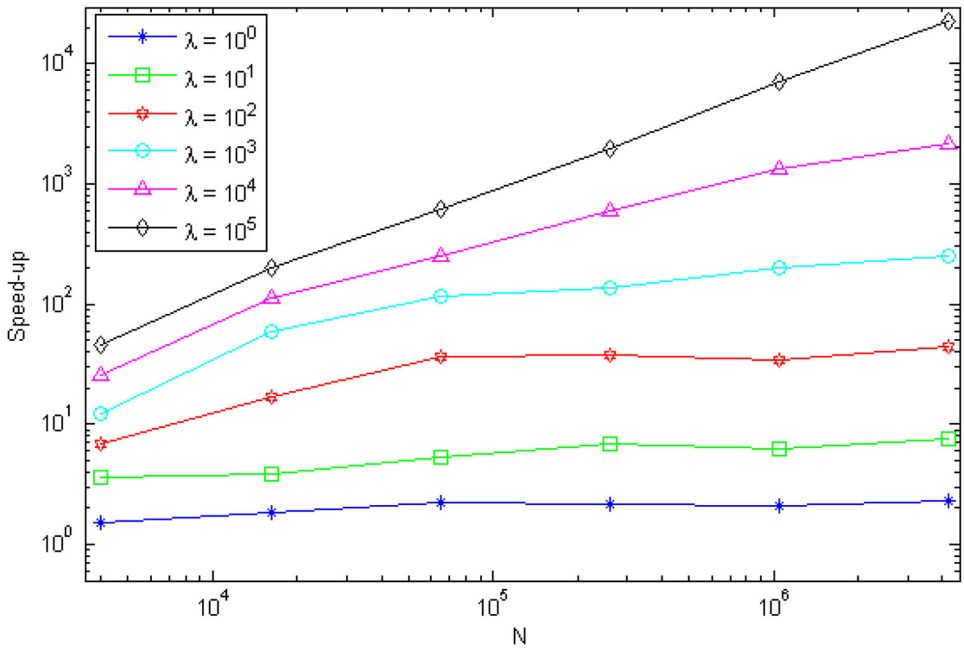

Figure 10. Speed-up for 1D problem.

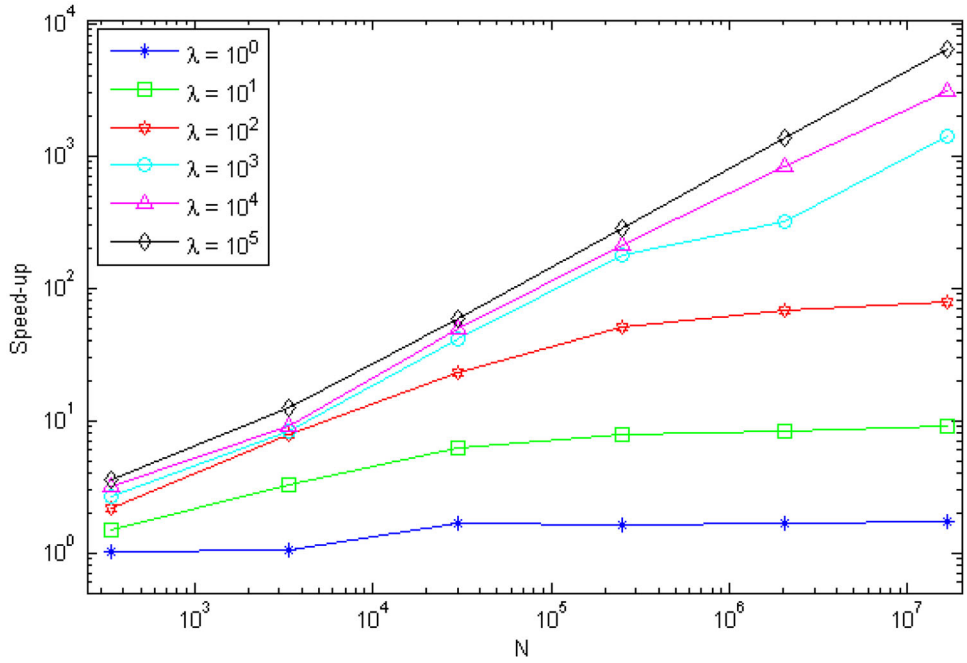

Figure 11. Speed-up for 2D problem.

4.6. Comments

The methodology presented here consists of using the time-stepping with multigrid method to solve the wave equation discretized by finite difference method. Similar results with the same efficiency can be obtained when considering external forces that operate on the problem, for example for the 1D case, just insert the term $F(x, t)$ on the right side of Eq. (1), because this causes changes only in the source term of the system of equations generated and according to Trottenberg et al. [14] it does not change the performance of the method.

There exist several works available in the literature showing the efficiency of the utilization of the time-stepping method combined with multigrid to solve EDPs, for example, in solving the Pennes bioheat equation in Stroher and Santiago [37], used to diagnose tumors non-invasively. The heat equation is also solved by combining the time-stepping method with multigrid in Lent [18]. In the work by Kumar et al. [38], a method to approximate the spread of uncertainties for the Richards equation is presented. It is also possible to verify the efficiency when using the time-stepping method with multigrid in the works of Gaspar et al. [39] and Luo et al. [40], where poroelasticity problems are solved numerically.

5. Final remarks

We have presented a scheme for solving one- and two-dimensional wave propagation problems, with discretization by the finite difference method, weighted by a parameter η at different time stages. We have obtained an implicit method of fourth-order for the one-dimensional problem and of second-order for the two-dimensional case, whenever $\tau_1 = h_1$ and $\tau_2 = h_x = h_y$. By utilizing the multigrid method with the lexicographical Gauss–Seidel solver in order to solve the resulting system of equations, we found discretization errors close to what we expected, at a lower computational time and linear complexity. The singlegrid method shows values of ρ very close to 1 when the value of λ is high, which implies a slow and less efficient process for this problem. On the other hand, the multigrid method proved to be very advantageous for this type of problem, because it has presented good convergence factors and showed robustness for the values of λ analyzed.

Disclosure statement

No potential conflict of interest was reported by the author(s).

Funding

This work was supported by Coordenação de Aperfeiçoamento de Pessoal de Nível Superior – Brazil grant 88882.381810/2019-01 and Universidade Federal do Paraná grant 75.095.679/0001-49.

ORCID

Maicon F. Malacarne http://orcid.org/0000-0003-3525-1750

Marcio A. V. Pinto http://orcid.org/0000-0003-4166-4674
Sebastião R. Franco http://orcid.org/0000-0002-4580-5924

References

[1] G. Avalos and I. Lasiecka, "Differential Riccati equation for the active control of a problem in structural acoustics," *J. Optim. Theory Appl.*, vol. 91, no. 3, pp. 695–728, 1996. DOI: 10.1007/BF02190128.

[2] A. Metaxas and R. J. Meredith, *Industrial Microwave Heating*. London, UK: IET, 1983.

[3] C. Bailly and D. Juve, "Numerical solution of acoustic propagation problems using linearized Euler equations," *AIAA J.*, vol. 38, no. 1, pp. 22–29, 2000. DOI: 10.2514/2.949.

[4] V. Gopal, R. Mohanty, and N. Jha, "New nonpolynomial spline in compression method of for the solution of 1D wave equation in polar coordinates," *Adv. Numer. Anal.*, vol. 2013, pp. 1–8, 2013. DOI: 10.1155/2013/470480.

[5] A. Brandt and I. Livshits, "Wave-ray multigrid method for standing wave equations," *Electron. Trans. Numer. Anal.*, vol. 6, pp. 162–181, 1997.

[6] V. Devi, R. K. Maurya, S. Singh, and V. K. Singh, "Lagrange's operational approach for the approximate solution of two-dimensional hyperbolic telegraph equation subject to Dirichlet boundary conditions," *Appl. Math. Comput.*, vol. 367, pp. e124717, 2020. DOI: 10.1016/j.amc.2019.124717.

[7] M. Dehghan and A. Mohebbi, "The combination of collocation, finite difference, and multigrid methods for solution of the two-dimensional wave equation," *Numer. Methods Partial Differ. Equ.*, vol. 24, no. 3, pp. 897–910, 2008. DOI: 10.1002/num.20295.

[8] M. A. Rincon and N. Quintino, "Numerical analysis and simulation for a nonlinear wave equation," *J. Comput. Appl. Math.*, vol. 296, pp. 247–264, 2016. DOI: 10.1016/j.cam.2015.09.024.

[9] H. M. Baskonus, H. Bulut, and T. A. Sulaiman, "New complex hyperbolic structures to the lonngren-wave equation by using sine-gordon expansion method," *Appl. Math. Nonlinear Sci.*, vol. 4, no. 1, pp. 129–138, 2019. DOI: 10.2478/AMNS.2019.1.00013.

[10] H. De Sterck, S. Friedhoff, A. J. Howse, and S. P. MacLachlan, "Convergence analysis for parallel-in-time solution of hyperbolic systems," *Numer. Linear Algebra Appl.*, vol. 27, no. 1, pp. e2271, 2020. DOI: 10.1002/nla.2271.

[11] M. J. Gander, L. Halpern, J. Rannou, and J. Ryan, "A direct time parallel solver by diagonalization for the wave equation," *SIAM J. Sci. Comput.*, vol. 41, no. 1, pp. A220–A245, 2019. DOI: 10.1137/17M1148347.

[12] M. J. Gander, F. Kwok, and B. C. Mandal, "Dirichlet–Neumann waveform relaxation methods for parabolic and hyperbolic problems in multiple subdomains," *BIT Numer. Math.*, vol. 61, no. 1, pp. 173–135, 2021. DOI: 10.1007/s10543-020-00823-2.

[13] J. A. Cuminato and M. Meneguette, *Discretization of Partial Differential Equations: Finite Difference Techniques* (in Portuguese). Rio de Janeiro, Brazil: Brazilian Mathematical Society, 2013.

[14] U. Trottenberg, C. W. Oosterlee, and A. Schuller, *Multigrid*. London, UK: Elsevier, 2000.

[15] R. Wienands and C. W. Oosterlee, "On three-grid fourier analysis for multigrid," *SIAM J. Sci. Comput.*, vol. 23, no. 2, pp. 651–671, 2001. DOI: 10.1137/S106482750037367X.

[16] W. L. Briggs, V. E. Henson, and S. F. McCormick, *A Multigrid Tutorial*. Philadelphia, PA: SIAM, 2000.

[17] N. Umetani, S. P. MacLachlan, and C. W. Oosterlee, "A multigrid-based shifted Laplacian preconditioner for a fourth-order Helmholtz discretization," *Numer. Linear Algebra Appl.*, vol. 16, no. 8, pp. 603–626, 2009. DOI: 10.1002/nla.634.

[18] J. Van Lent , Multigrid Methods for Time-Dependent Partial Differential Equations. Leuven: Katholieke Universiteit Leuven, 2006.

[19] B. Ji, H.-L. Liao, Y. Gong, and L. Zhang, "Adaptive second-order Crank–Nicolson time-stepping schemes for time-fractional molecular beam epitaxial growth models," *SIAM J. Sci. Comput.*, vol. 42, no. 3, pp. B738–B760, 2020. DOI: 10.1137/19M1259675.

[20] H.-L. Liao, T. Tang, and T. Zhou, "A second-order and nonuniform time-stepping maximum-principle preserving scheme for time-fractional Allen-Cahn equations," *J. Comput. Phys.*, vol. 414, pp. e109473, 2020. DOI: 10.1016/j.jcp.2020.109473.

[21] M. Chen, S. Zhang, S. Li, X. Ma, X. Zhang, and Y. Zou, "An explicit algorithm for modeling planar 3D hydraulic fracture growth based on a super-time-stepping method," *Int. J. Solids Struct.*, vol. 191–192, pp. 370–389, 2020. DOI: 10.1016/j.ijsolstr.2020.01.011.

[22] J. C. Tannehill , D. A. Anderson and R. H. Pletcher, *Computational Fluid Mechanics and Heat Transfer*. Philadelphia, PA: Taylor & Francis,1997.

[23] P. J. Olver, Introduction to Partial Differential Equations. New York, USA: Springer, 2014.

[24] R. Burden and J. Faires, *Numerical Analysis*. Boston: Brooks/Cole Cengage Learning, 2016.

[25] A. Brandt and O. E. Livne, *Multigrid Techniques: 1984 Guide with Applications to Fluid Dynamics*, revised ed. SIAM, 2011. DOI: 10.1137/1.9781611970753.

[26] P. Wesseling, "Introduction to Multigrid Methods," Technical Report. Institute for Applications in Science and Engineering, Hampton, VA, 1995.

[27] S. R. Franco, F. J. Gaspar, M. A. V. Pinto, and C. Rodrigo, "Multigrid method based on a space-time approach with standard coarsening for parabolic problems," *Appl. Math. Comput.*, vol. 317, pp. 25–34, 2018. DOI: 10.1016/j.amc.2017.08.043.

[28] M. A. V. Pinto, C. Rodrigo, F. J. Gaspar, and C. Oosterlee, "On the robustness of ilu smoothers on triangular grids," *Appl. Numer. Math.*, vol. 106, pp. 37–52, 2016. DOI: 10.1016/j.apnum.2016.02.007.

[29] H. C. Elman, O. G. Ernst, and D. P. O'leary, "A multigrid method enhanced by Krylov subspace iteration for discrete Helmholtz equations," *SIAM J. Sci.*

Comput., vol. 23, no. 4, pp. 1291–1315, 2001. DOI: 10.1137/S1064827501357190.

[30] T. C. Clevenger, T. Heister, G. Kanschat, and M. Kronbichler, "A flexible, parallel, adaptive geometric multigrid method for fem," *arXiv preprint arXiv*:1904.03317, 2019.

[31] M. L. Oliveira, M. A. V. Pinto, S. F. T. Gonçalves, and G. V. Rutz, "On the robustness of the xy-zebra-gauss-seidel smoother on an anisotropic diffusion problem," *Comput. Model. Eng. Sci.*, vol. 117, no. 2, pp. 251–270, 2018.

[32] S. R. Franco, C. Rodrigo, F. J. Gaspar, and M. A. V. Pinto, "A multigrid waveform relaxation method for solving the poroelasticity equations," *Comput. Appl. Math.*, vol. 37, no. 4, pp. 4805–4820, 2018. DOI: 10.1007/s40314-018-0603-9.

[33] M. Adams, M. Brezina, J. Hu, and R. Tuminaro, "Parallel multigrid smoothing: polynomial versus Gauss–Seidel," *J. Comput. Phys.*, vol. 188, no. 2, pp. 593–610, 2003. DOI: 10.1016/S0021-9991(03)00194-3.

[34] C. H. Marchi and A. F. C. Silva, "Multi-dimensional discretization error estimation for convergent apparent order," *J. Braz. Soc. Mech. Sci. Eng.*, vol. 27, no. 4, pp. 432–439, 2005. DOI: 10.1590/S1678-58782005000400012.

[35] G. Horton and S. Vandewalle, "A space-time multigrid method for parabolic partial differential equations," *SIAM J. Sci. Comput.*, vol. 16, no. 4, pp. 848–864, 1995. DOI: 10.1137/0916050.

[36] C.-A. Thole and U. Trottenberg , "Basic smoothing procedures for the multigrid treatment of elliptic 3D-operators," in *Advances in multi-grelha Methods* ,Springer, Wiesbaden, 1985, pp.102–111.

[37] G. R. Stroher and C. D. Santiago, "Numerical two-dimensional thermal analysis of the human skin using the multigrid method," *Acta Sci. Technol.*, vol. 42, pp. e40992, 2019. DOI: 10.4025/actascitechnol.v42i1.40992.

[38] P. Kumar, C. Rodrigo, F. J. Gaspar, and C. W. Oosterlee, "A parametric acceleration of multilevel monte carlo convergence for nonlinear variably saturated flow," *Comput. Geosci.*, vol. 24, no. 1, pp. 311–331, 2020. DOI: 10.1007/s10596-019-09922-8.

[39] F. J. Gaspar, F. J. Lisbona, C. W. Oosterlee, and R. Wienands, "A systematic comparison of coupled and distributive smoothing in multigrid for the poroelasticity system," *Numer. Linear Algebra Appl.*, vol. 11, no. 2–3, pp. 93–113, 2004. DOI: 10.1002/nla.372.

[40] P. Luo, C. Rodrigo, F. J. Gaspar, and C. Oosterlee, "On an uzawa smoother in multigrid for poroelasticity equations," *Numer. Linear Algebra Appl.*, vol. 24, no. 1, pp. e2074, 2017. DOI: 10.1002/nla.2074.